Astron. Astrophys. 61, 515—521 (1977)

ASTRONOMY AND ASTROPHYSICS

Theoretical Stellar Chromospheres of Late Type Stars II.

II. Temperature Minima

P. Ulmschneider[1], F. Schmitz[1], A. Renzini[2], C. Cacciari[2], W. Kalkofen[3] and R. Kurucz[3]

[1] Institut für Astrophysik, Universität Würzburg, D-8700 Würzburg, Federal Republic of Germany
[2] Osservatorio Astronomico Universitario, Bologna, Italy
[3] Center for Astrophysics, Cambridge, Mass. 02138 USA

Received January 28; revised April 7, 1977

Summary. We apply the theory of heating by short period acoustic waves to predict the height of shock formation and the acoustic flux at the base of the chromosphere for stars with $T_{\rm eff}=4000$ to 6500 K and log $g=2$ to 4. These predictions are compared with heights of temperature minima and with chromospheric radiation losses computed from semiempirical models.

Key words: acoustic heating — temperature minimum — stellar chromosphere

I. Introduction

In this second of a series of papers on theoretical chromospheres of late type stars we use the short period acoustic heating theory for a more detailed prediction of the height of stellar temperature minima. This is essentially an extension of our work on the sun (Ulmschneider et al., 1977; Kalkofen and Ulmschneider, 1977; Ulmschneider and Kalkofen, 1977). Using values of the acoustic flux and period obtained from a convection zone calculation (Renzini et al., 1977, henceforth called Paper I) we follow the development of the radiatively damped acoustic wave until shock formation. The acoustic waves propagate through LTE radiative equilibrium stellar atmosphere models, described in Section 2. In Section 3 we discuss the results of the wave computations, the height of shock formation, and the amount of acoustic flux that remains at this height. In Section 4 we consider the relationship between the height of shock formation and the temperature minimum, and give a comparison of our results with values of both the temperature minimum height and the chromospheric radiation flux that are derived from observation by other authors. Because of numerical difficulties several important changes of our original method were made; they are discussed in the Appendix.

Send offprint requests to: P. Ulmschneider

II. Radiative Equilibrium Atmospheres

Ideally, we would like to determine the mean atmospheric structure of the shock heated atmosphere from a self-consistent solution of the mass, momentum and energy conservation equations. Unfortunately, it is not technically feasible to solve the relevant equations: in particular it is impossible to solve for every time step the radiation transfer equations at sufficient frequencies to satisfactorily account for line blanketing and non-LTE effects. To overcome this problem (Ulmschneider and Kalkofen, 1977), we have separated the calculation into two parts: we first construct radiative equilibrium models including an accurate treatment of line blanketing (we have not yet considered non-LTE transfer problems), and then we propagate acoustic waves into this model using a grey (one frequency point), LTE approximation to compute the radiation transfer. This method is a fairly crude approximation, but it retains the advantages of the high refinement of state-of-the-art radiative and hydrostatic equilibrium models, while allowing a computationally feasible attack on the hydrodynamic problem. We should emphasise that the hydrodynamic problem is solved as a "perturbation", so that the grey approximation may be a good approximation to the perturbation radiation losses which are presumably dominated by continuum processes. We consider 14 stellar models with effective temperatures ranging from $T_{\rm eff}=4000$ to 6500 K and surface gravities from log $g=2$ to 4. Some of these models (labelled with an asterisk in the second column of Table 1) are non-grey LTE radiative equilibrium models that have been computed by Kurucz (1977) using the ATLAS code (Kurucz, 1970). These models include theoretical opacities for a large number of atomic lines and take into account convective flux under the assumption that the ratio of the mixing length to the pressure scale height has the value $\alpha=2.0$. A value of 2 km s^{-1} was used for the microturbulent velocity. For the remaining models (indicated by a plus sign in the second column of Table 1), we use those of Carbon and Gingerich (1969). These

Table 1. Stellar parameters, effective temperature $T_{\rm eff}$, surface gravity g, mechanical flux πF_M, acoustic period P and physical parameters at the point of shock formation, monochromatic optical depth τ at 0.5 μm, gas pressure p, temperature T, geometrical height x and maximum velocity amplitude v. The ratio α of mixing length and pressure scale height is 1.0. Values in parentheses are for calculations without radiative damping. Photospheric models of Carbon and Gingerich (1969) are labeled by +, those of Kurucz (1977) by *

$T_{\rm eff}$ (K)	log g (cm/s^2)	πF_M (erg/cm^{2}s)	P (s)	τ	p (dyn/cm^2)	T (K)	x (cm)	v (cm/s)
4000	+4	3.37 E 5	6.43 E 1	8.0 E-8	1.3 E 1	3150	2.0 E 8	6.4 E 4
				(4.2 E-7)	(5.4 E 1)	(3170)	(1.7 E 8)	(6.6 E 4)
	+3	1.93 E 6	6.67 E 2	7.2 E-6	6.9 E 1	3210	1.4 E 9	6.4 E 4
				(5.2 E-5)	(2.7 E 2)	(3230)	(1.1 E 9)	(7.2 E 4)
	+2	8.02 E 6	6.89 E 3	9.3 E-4	3.6 E 2	3260	7.3 E 9	5.8 E 4
				(4.1 E-3)	(9.1 E 2)	(3300)	(5.4 E 9)	(7.9 E 4)
4500	+4	1.60 E 6	6.79 E 1	8.2 E-7	5.1 E 1	3500	1.9 E 8	6.2 E 4
				(1.0 E-5)	(2.3 E 2)	(3550)	(1.5 E 8)	(7.2 E 4)
	+3	7.39 E 6	7.06 E 2	1.6 E-4	3.0 E 2	3600	1.2 E 9	5.9 E 4
				(9.0 E-4)	(8.0 E 2)	(3640)	(9.1 E 8)	(8.3 E 4)
5000	+4	5.68 E 6	7.00 E 1	3.8 E-6	1.0 E 2	3940	1.8 E 8	6.4 E 4
				(1.4 E-4)	(7.7 E 2)	(4020)	(1.4 E 8)	(7.6 E 4)
	+3	2.29 E 7	7.18 E 2	1.2 E-3	7.0 E 2	4090	1.0 E 9	6.1 E 4
				(9.5 E-3)	(2.2 E 3)	(4180)	(7.5 E 8)	(9.1 E 4)
	+2	1.27 E 8	7.45 E 3	3.6 E-1	4.3 E 3	4840	1.8 E 9	1.4 E 5
				(3.7 E-1)	(4.3 E 3)	(4840)	(1.8 E 9)	(1.6 E 5)
5500	+4	1.64 E 7	7.24 E 1	4.2 E-5	3.7 E 2	4430	1.7 E 8	6.3 E 4
				(9.0 E-4)	(2.0 E 3)	(4510)	(1.2 E 8)	(8.3 E 4)
	+3	7.74 E 7	7.44 E 2	1.9 E-2	3.0 E 3	4650	6.5 E 8	7.5 E 4
				(5.3 E-2)	(5.2 E 3)	(4780)	(4.9 E 8)	(1.4 E 5)
5770	4.44	1.59 E 7	2.69 E 1	2.2 E-5	4.9 E 2	4030	6.2 E 7	6.6 E 4
				(3.2 E-4)	(2.1 E 3)	(4280)	(4.7 E 7)	(7.8 E 4)
6000	* 4	4.38 E 7	7.56 E 1	2.8 E-4	1.0 E 3	4580	1.6 E 8	7.6 E 4
				(3.9 E-3)	(4.3 E 3)	(4800)	(8.0 E 7)	(9.4 E 4)
	* 3	2.57 E 8	7.68 E 2	1.9 E-1	8.5 E 3	5520	1.8 E 8	1.7 E 5
				(1.9 E-1)	(8.5 E 3)	(5520)	(1.8 E 8)	(1.7 E 5)
6500	* 4	1.41 E 8	7.77 E 1	5.0 E-3	4.3 E 3	5220	8.0 E 7	7.8 E 4
				(2.3 E-2)	(9.7 E 3)	(5390)	(5.5 E 7)	(1.2 E 5)

models take empirical distribution functions for the line opacities that were derived from observations of Arcturus, Procyon and the Sun. To study the influence of the choice of the equilibrium model on a theoretical chromosphere a few models of Carbon and Gingerich were recomputed with the ATLAS code.

Some of the photospheric models do not extend as high as the point of shock formation. These models were extended smoothly but somewhat arbitrarily, assuming a boundary temperature of $T_0 = 3000$ K. At great geometrical height x, we assumed the temperature (in K) as given by the relation

$$T = 3000\,(1 + A e^{-Bx}), \tag{1}$$

where A and B are constants determined by the last few points of the photospheric model.

The final photospheric models thus chosen represent a considerable source of uncertainty. Not only have non-LTE effects in the lines and continua (for a discussion whether Cayrel heating or cooling applies, see Kalkofen, 1977) been neglected but for about one third of the 14 models (see Tables 1 and 2) the photospheric range had to be extended arbitrarily in precisely those regions where the shocks form. In addition uncertainties are introduced by inconsistencies in the assumptions entering the photospheric models at the one hand and the stellar interior calculations employing Cox opacities and values of α between 1.0 and 1.5 at the other hand. A detailed evaluation of these errors is at the moment beyond the scope of this work and will not be attempted.

III. Results

a) Wave Computation

The method of computation of acoustic waves in a stellar atmosphere with the perturbation approach and the grey approximation has been described by Ulmschneider and Kalkofen (1977) and will not be repeated here. The wave is introduced through excitation of the lower boundary of the atmosphere by a piston. The velocity u of the piston is determined by the total acoustic flux πF_M and the acoustic period P using

$$u = -u_0 \sin\left(\frac{2\pi}{P}\,t\right), \tag{2}$$

Table 2. As in Table 1, with $\alpha=1.5$

$T_{\rm eff}$ (K)	log g (cm/s^2)	πF_M (erg/cm^{2}s)	P (s)	τ	p (dyn/cm^2)	T (K)	x (cm)	v (cm/s)
4000	+4	8.22 E 5	5.58 E 1	4.6 E-7	5.2 E 1	3170	1.7 E 8	5.2 E 4
				(2.1 E-6)	(1.5 E 2)	(3180)	(1.5 E 8)	(6.8 E 4)
	+3	5.28 E 6	6.53 E 2	5.0 E-5	2.6 E 2	3230	1.1 E 9	5.3 E 4
				(3.0 E-4)	(7.2 E 2)	(3240)	(8.8 E 8)	(7.2 E 4)
	+2	2.62 E 7	6.79 E 3	8.9 E-3	1.4 E 3	3340	4.5 E 9	5.8 E 4
				(2.4 E-2)	(2.4 E 3)	(3410)	(3.4 E 9)	(8.9 E 4)
4500	+4	4.00 E 6	6.76 E 1	5.4 E-6	1.6 E 2	3540	1.6 E 8	5.6 E 4
				(4.0 E-5)	(5.8 E 2)	(3580)	(1.3 E 8)	(7.2 E 4)
	+3	2.30 E 7	6.80 E 1	9.5 E-4	8.0 E 2	3640	9.1 E 8	5.6 E 4
				(6.0 E-3)	(2.5 E 3)	(3710)	(6.6 E 8)	(8.2 E 4)
5000	+4	1.64 E 7	6.89 E 1	2.9 E-5	3.2 E 2	3980	1.6 E 8	6.1 E 4
				(8.5 E-4)	(2.2 E 3)	(4070)	(1.1 E 8)	(7.7 E 4)
	+3	7.45 E 7	6.94 E 2	1.1 E-2	2.3 E 3	4190	7.3 E 8	6.4 E 4
				(5.5 E-2)	(5.7 E 3)	(4370)	(4.9 E 8)	(1.0 E 5)
	+2	3.16 E 8	7.21 E 3	6.1 E-1	5.5 E 3	5100	9.5 E 8	2.0 E 5
				(8.7 E-1)	(6.4 E 3)	(5330)	(4.6 E 8)	(2.5 E 5)
5500	+4	5.16 E 7	7.13 E 1	4.1 E-4	1.3 E 3	4490	1.3 E 8	6.2 E 4
				(5.7 E-3)	(5.5 E 3)	(4570)	(8.7 E 7)	(8.8 E 4)
	+3	2.10 E 8	7.20 E 2	1.7 E-1	9.7 E 3	5010	2.9 E 8	1.2 E 5
				(1.8 E-1)	(1.0 E 4)	(5020)	(2.8 E 8)	(1.4 E 5)
5770	4.44	4.91 E 7	2.60 E 1	2.1 E-4	1.7 E 3	4230	5.0 E 7	5.7 E 4
				(2.5 E-3)	(6.2 E 3)	(4500)	(3.6 E 7)	(8.0 E 4)
6000	* 4	1.37 E 8	7.31 E 1	3.3 E-3	4.0 E 3	4800	8.2 E 7	6.9 E 4
				(2.2 E-2)	(1.1 E 4)	(5000)	(5.9 E 7)	(1.1 E 5)
	* 3	6.87 E 8	7.44 E 2	7.5 E-1	1.3 E 4	6350	2.0 E 6	2.3 E 5
				(7.5 E-1)	(1.3 E 4)	(6350)	(2.0 E 6)	(2.3 E 5)
6500	* 4	3.51 E 8	7.53 E 1	3.8 E-2	1.2 E 4	5490	4.7 E 7	9.5 E 4
				(8.2 E-2)	(1.8 E 4)	(5650)	(3.4 E 7)	(1.4 E 5)

where the velocity amplitude u_0 is given by

$$u_0=\left(\frac{2\pi F_M}{\rho c}\right)^{1/2}. \quad (3)$$

Here ρ is the density and c the sound velocity at the lower boundary of the atmosphere. The values for the acoustic flux πF_M and the period P have been taken from Paper I and are listed in Tables 1 and 2. The period P is that of the maximum of the acoustic frequency spectrum. The acoustic flux and, to a lesser degree, the period depend on the parameter α, the ratio of the mixing length to the pressure scale height, which is a crucial parameter in the calculation of a convection zone.

The lower boundary was taken at optical depth greater than $\tau_{5000}=100$ to ensure that the perturbed outgoing intensity I^{1+} may safely be set equal to zero. A more reasonable position of the piston would be between $\tau=1$ and 10, just above the layer where most of the acoustic flux is generated. However by introducing the total acoustic flux at a lower layer where radiative damping is unimportant we avoid a detailed prescription of I^{1+}. The grid size and time step were chosen as described by Ulmschneider and Kalkofen (1977). As discussed in the Appendix the computational method has been modified to overcome difficulties that did not appear in the solar case.

b) Height of Shock Formation

Figure 1 shows the Eulerian height of shock formation as a function of the effective temperature $T_{\rm eff}$ with the surface gravity g as a parameter. The height coordinate is a mass column density (in g/cm^2) defined by

$$m=\frac{p}{g}, \quad (4)$$

where p is the gas pressure. The relation of this height to the temperature minimum is discussed in Section 4. Also shown in Figure 1 is the height of shock formation (dashed) found when the wave does not suffer radiative damping. The heights for adiabatic waves are roughly 1 to 1.5 pressure scale heights smaller than those for the radiatively damped waves. If purely radiative causes for a temperature rise are excluded, an assumption which we make everywhere in the present work, the heights of shock formation of adiabatic waves give lower limits for the location of the temperature minimum.

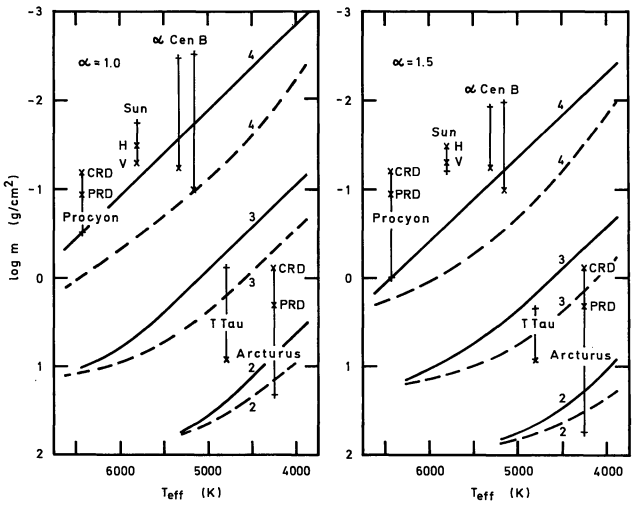

Fig. 1. Height of shock formation on a mass column density as a function of $T_{\rm eff}$ with $\log g$ as parameter. α is the ratio of mixing length to pressure scale height. + marks shock heights for individual stars. × gives the semi-empirical height for the temperature minimum of these stars. CRD and PRD refer to complete and partial redistribution, see text. H is the HSRA and V the VAL temperature minimum. Shock heights for undamped waves are shown dashed.

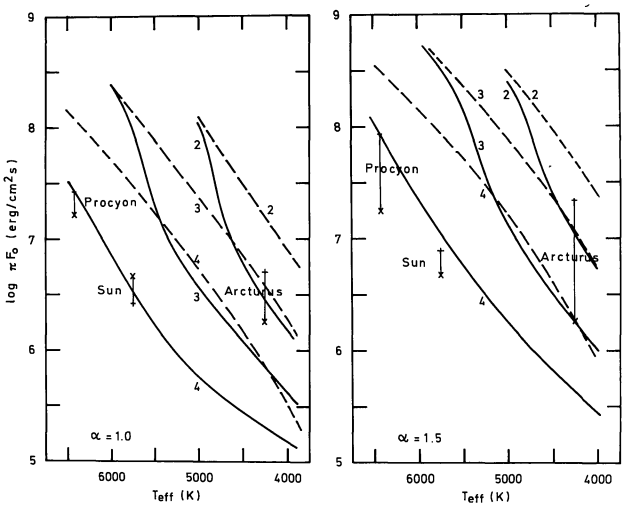

Fig. 2. Acoustic flux πF_0 at shock formation as a function of $T_{\rm eff}$ with $\log g$ as parameter. α is the ratio of mixing length to pressure scale height. + marks the acoustic flux for individual stars. × gives values of chromospheric emission of these stars determined by Ayres. Initial acoustic flux πF_M generated in the convection zone is shown dashed

Upper limits are given by the height of the sonic point, which is defined (see Paper I) as the height where the velocity amplitude of an adiabatic wave becomes equal to the sound velocity. The height of the sonic point was generally found to be about 3 scale heights larger than the height for radiatively damped waves.

As may be seen in Figure 1, the height of shock formation decreases with increasing $T_{\rm eff}$ and decreasing gravity. This is due to the increased mechanical flux which leads to larger wave amplitudes, greater nonlinear effects and hence earlier shock formation. The physical state at the point of shock formation is shown in Tables 1 and 2. At high $T_{\rm eff}$ and low gravity, the points of shock formation are found in the radiative damping zone. Thus, in these cases the shock heights for damped waves approach those of the adiabatic waves (cf. Fig. 1).

c) Acoustic Flux at Shock Formation

Figure 2 shows the mechanical flux πF_0 remaining in the wave at the point of shock formation. Also shown is the total acoustic flux πF_M predicted in Paper I. For stars with high effective temperature and low surface gravity, the final flux πF_0 approaches the initial flux πF_M since the height of shock formation lies in the radiative damping zone.

d) Influence of the Choice of Radiative Equilibrium Model

To test the influence of the choice of the radiative equilibrium models, we computed shock heights for models with $T_{\rm eff}=5500$ K and $\log g=3$ and 4 using the models of both Carbon and Gingerich (1969) and Kurucz (1977). The minimum temperature in the Kurucz models was found to be lower by 60 K for $\log g=3$ and by 200 K for $\log g=4$. The pressure and geometrical height above $\tau_{5000}=1$ of the shock formation point differed by less than 5% between the two sets of models.

IV. Discussion

a) Relation of Shock Formation Height and Temperature Minimum

Our calculations for the sun (Ulmschneider and Kalkofen, 1977) have shown that the short period acoustic heating theory offers an explanation for the temperature minimum and the chromospheric temperature rise. As discussed recently by Praderie and Thomas (1976), by Ulmschneider and Kalkofen (1977) and by Cram (1977), there are still many uncertainties associated with this theory. Aside from uncertainties in the theory of acoustic energy generation, discussed in Paper I, there is the problem of how well a one-dimensional calculation is able to predict the observed position of the temperature minimum which, because of the inhomogeneous nature of the solar surface layers, can only be an averaged position. Important effects such as acoustic refraction and enhanced energy generation in network regions are not included in our calculations. Another basic problem is the relation of the observed temperature minimum with the point of shock formation. The rate of energy dissipation by the wave will increase rapidly in the layers between the height of shock formation

and the height where the shock becomes fully-developed. Unless there is a radiatively induced temperature reversal below these heights, it appears reasonable to hypothesise that the chromospheric temperature rise will begin here, where the rate of energy dissipation increases rapidly. The possibility of a radiatively induced temperature inversion was proposed by Cayrel (1963, 1964), but the relative importance of this process, line blanketing, and mechanical heating has not yet been clarified, even for the solar atmosphere (Kalkofen, 1977; Cram, 1977). We would like to have some way to compare our theoretical calculations with observed properties of stellar chromospheres, and in the absence of a refined theory for the structure of stellar temperature minima we provisionally identify the point of shock formation with the temperature minimum.

b) Comparison of Shock Formation Heights with Empirical Temperature Minima

In Figure 1 we have compared our theoretical predictions of the height of shock formation with semi-empirical determinations of the position of the temperature minima in Arcturus, Procyon, α Cen B and the Sun. The height of shock formation for the Sun was determined using the modified HSRA model described by Ulmschneider and Kalkofen (1977; the small change from the previous results are due to differences in the shock finding procedure). The positions of the temperature minima of the HSRA model (labelled H) and the Vernazza et al. (1976) model (labelled V) are indicated: the good agreement between theoretical and semi-empirical temperature minima for the Sun was discussed by Ulmschneider and Kalkofen (1977). The positions of the stellar temperature minima have been determined by Ayres et al. (1974), Ayres and Linsky (1975), Ayres et al. (1976) mainly by adjusting atmospheric models to produce theoretical Ca II H and K and Mg II *h* and *k* lines in agreement with observations. The heights of the semi-empirical temperature minima have been found to decrease if instead of complete redistribution (CRD) a more appropriate partial redistribution (PRD) is assumed for the line formation (Ayres and Linsky, 1975). Note that this improvement moves the semi-empirical heights closer to our theoretical values.

In Figure 1, two entries were made for α Cen B because of uncertain stellar parameters (Ayres et al., 1976). For Arcturus a detailed hydrodynamic computation would very likely give a greater height for the temperature minimum since the shock is formed in the radiative damping zone (see Section 4a).

The positions of empirical temperature minima have also been determined for T-Tauri stars. Herbig (1969; see also Dumont et al., 1973) suggested that the observed T-Tauri emission spectrum may be explained by a chromosphere reaching down to about $\tau_{5000}=0.25$. Assuming an opacity $\varkappa$ of about 0.03 cm^2/g (Carbon and Gingerich, 1969, pp. 436, 438), we find for the location of the temperature minimum values of the mass $m \approx \tau/\varkappa$ of about 8 g/cm^2. Here $T_{\rm eff}=4800$ and log $g=2.9$ was assumed for T-Tauri (Schwartz, 1974). A comparison between Herbig's suggested and our theoretically inferred temperature minimum is shown in Figure 1.

c) Comparison of the Acoustic Flux at Shock Formation with Empirical Chromospheric Emission

If short period acoustic shock waves are the main heating mechanism in a stellar chromosphere then acoustic waves at the temperature minimum must carry enough energy to balance the main part of the chromospheric emission. Thus, a comparison of the acoustic energy at shock formation and of the chromospheric radiation loss computed from semi-empirical models can be taken as an independent test for the validity of the short period acoustic heating theory. In Figure 2 we have plotted the semi-empirical chromospheric emission πF_0 of the Sun, Arcturus and Procyon given by Ayres (1975, p. 129). The good agreement of theoretical and semi-empirical values of the flux πF_0 for the Sun has already been discussed elsewhere (Ulmschneider and Kalkofen, 1977). Due to the different shock finding procedure in the present work, especially in the limit of zero grid size at shock formation, the fluxes πF_0 for the Sun are slightly different from our earlier values. We find $\pi F_0=2.7$ E6 and 7.8 E6 erg/cm^{2}s for $\alpha=1.0$ and 1.5, respectively.

For Procyon, the discrepancy between observed and predicted chromospheric fluxes is of the same order of magnitude as that for the Sun. In Arcturus the shock forms in the radiative damping zone. One would expect, therefore, that the temperature minimum lies above the shock formation point. As the acoustic wave moves from the shock formation point to the temperature minimum where it is a fully developed shock, it loses more energy through radiative damping so that the energy remaining in the wave is less than what it was at the shock formation point. Thus the amount of acoustic energy available to heat the chromosphere is less than πF_0, and the discrepancy between estimated and observed chromospheric fluxes should be much smaller than is indicated in Figure 2.

Appendix

a) Large Temperature Gradients

Due to the large temperature gradients in the photospheres of stars of high $T_{\rm eff}$ and low gravity, velocity amplitudes of considerable size (spikes) appeared spontaneously in the region of largest temperature gradient of the unperturbed atmosphere. Difficulties of this type are well known (Klein et al., 1975) and appear if the

initial, static atmosphere has not been computed with the same code as the dynamical atmosphere. In contrast to the finite difference scheme, an initial atmosphere that shows no time dependence can usually not be constructed with the modified characteristics method. This may be seen as follows. Consider a grid with a constant step size having N height points. In a static atmosphere with prescribed temperature structure the N values of the fluid velocity u, with $u=0$, and of the initial sound velocity c are known. Because the entropy is known up to an additive constant only $N-1$ values of the entropy remain to be determined (Ulmschneider et al., 1977). Since two characteristics C^+ and C^- emanate from each interior point, and one emanates from each boundary point we have $2N-2$ differential equations for only $N-1$ unknowns. This overdetermination is avoided by choosing grid points separated by the distances over which sound travels in the fixed time interval Δt. Then, characteristics intersect at grid points. However the time step Δt cannot be kept fixed, since Δt is determined by the Courant condition and by radiative relaxation. Thus the only way to overcome the difficulties associated with the spikes is to reduce the grid size. We found a reduction of the grid distance by a factor of 2 decreased the amplitude of the spikes by a factor of about 4.

b) Shockfinding

The method of shockfinding described by Ulmschneider et al. (1976), henceforth called the old method, worked well for adiabatic cases and for the Sun, but it did not find the correct shock position for stars with high $T_{\rm eff}$ and low g. We decided to follow pairs of C^+ characteristics from the piston boundary up to their intersection point, where the shocks appear. If the timestep at time $t=0$ is $\Delta t'$ we took series of C^+ characteristics that were separated by $\Delta t'/4$ and entered from the piston boundary at times between $t=1/4\ P$ and $3/4\ P$, where P is the wave period. For pairs of this set of characteristics separated by $t=\Delta t'/4$, $\Delta t'/2$ and $\Delta t'$ the intersection points were determined using Stefanik's method (Ulmschneider et al., 1977). For each separation the intersection points for the shortest time interval were selected. By decreasing the grid distance we found that these intersection points converged to a common point in the a, t diagram. In the cases without radiative damping and in stars of low g this point agreed with the point found by the old method. In the case without radiative damping this point was checked against the exact shock formation point computed with the full characteristics method. This method, which cannot be employed for problems that include radiation because it does not advance the solution by constant time steps, may easily be adopted for adiabatic acoustic wave calculations. It is easy to program (Smith, 1970) and is between 3 and 6 times faster than the modified method of characteristics. Thus in order to determine a shock position exhibited in Figure 1 and Tables 1 and 2 we performed all calculations twice, using grid distance Δa and $1/2\ \Delta a$ and extrapolated to $\Delta a=0$.

c) Interpolation

With a simple parabolic interpolation, oscillations sometimes appear in the compression region of the wave, especially in cases of high $T_{\rm eff}$ and low g. These oscillations are similar to the double peaks found in the calculations of Ulmschneider et al. (1977). It is important to realize that these oscillations are fundamentally different from oscillations found in finite difference methods which arise from improper treatment of shock dissipation and which are usually damped out using artificial viscosity. In our case, these oscillations result exclusively from the use of the parabolic interpolation in the modified characteristics method. Consider, for instance, velocity amplitudes u_1, u_2, u_3, u_4 at grid points a_1, a_2, a_3, a_4. If u_1, u_2 and u_3 are large and u_4 is small, as occurs near a shock, parabolic interpolation will result in a large overshoot of u between a_2 and a_3. We avoid this by a more suitable interpolation scheme using a weighted mean of forward and backward parabolas as in the ATLAS code (Kurucz, 1970). For a value of a between the points a_2 and a_3 we compute the velocity u using a mean parabola,

$$u=c_1+c_2a+c_3a^2, \tag{5}$$

where the coefficients c_1, c_2, c_3 are computed from two parabolas $c_{11}+c_{21}a+c_{31}a^2$ and $c_{12}+c_{22}a+c_{32}a^2$ through the u values at points a_1, a_2, a_3 and a_2, a_3, a_4, respectively, with

$$c_k=c_{k1}w+c_{k2}(1-w) \tag{6}$$

for $k=1, 2, 3$ and where

$$w=|c_{32}|/(|c_{31}|+|c_{32}|). \tag{7}$$

With this interpolation no oscillations were found. A comparison with the result of computations using the full characteristics method and with the exact simple wave solution showed excellent agreement.

d) Timestep Due to Radiative Relaxation

As described by Kalkofen and Ulmschneider (1977) we have employed two criteria to selected the timestep. One was the usual Courant condition and the other a condition on the maximum allowed change of entropy caused by radiation damping. Usually, as in the solar case, the Courant condition was the more restrictive criterion for the timestep. For stars with high $T_{\rm eff}$ and low g, however, the timestep was determined mainly by the radiative relaxation time which for our purpose is the time in which a gas element suffers the maximum

allowed entropy change. The actual timestep of the computation should always be smaller than the relaxation time. We have accomplished this by monitoring the convergence of the iteration on the entropy change D (Kalkofen and Ulmschneider, 1977). In the D iteration, convergence is considered to be achieved if at every point

$$(|D_{\mathrm{Old}}| - |D_{\mathrm{New}}|)/|D_{\mathrm{Max}}| < \varepsilon. \tag{8}$$

Here ε is approximately 0.01 and $|D_{\mathrm{Max}}|$ is the absolute maximum of the radiative damping function D. We selected three indices $i_1 = 5$, $i_2 = 8$ and $i_3 = 12$. When the number of the D-iterations until convergence, i_D, is less than i_1 we increase the timestep by 10%. If this violates the Courant condition the timestep is not changed. If i_D is greater than i_2 we decrease the timestep by 10%. Finally if i_D is greater than i_3 we consider convergence not achieved, decrease the timestep by 25%, and step back to repeat the iteration. Only in a few cases, usually at the start of a calculation, was the timestep significantly smaller than the Courant timestep.

Acknowledgements. We want to acknowledge extensive discussions with Dr. L. Cram, who helped considerably to clarify difficult parts of this work.

Note added in proof: Recent work by Cram and Ulmschneider (1977, *Astron. Astrophys.*, in press) has shown that the identification of the height of shock formation with the height of the temperature minimum valid for solar type stars is very likely incorrect for stars of high T_{eff} and low gravity. In these cases radiation damping of the developing shock wave most likely will increase the height of the temperature minimum above the shock formation height. This will also lead to a considerable decrease of the acoustic flux πF_0 at the temperature minimum compared with the values published in this work.

References

Ayres, T. R., Linsky, J. L., Shine, R. A.: 1974, *Astrophys. J.* **192**, 93
Ayres, T. R.: 1975, Ph. D. Thesis, University of Colorado, Boulder
Ayres, T. R., Linsky, J. L.: 1975, *Astrophys. J.* **200**, 660
Ayres, T. R., Linsky, J. L., Rodgers, A. W., Kurucz, R. L.: 1976 *Astrophys. J.* **210**, 199
Carbon, D. F., Gingerich, O.: 1969, Proc. 3rd Harvard Conf. on Stellar Atmospheres, MIT Press, Cambridge
Cayrel, R.: 1963, *Compt. Rend. Acad. Sci. Paris* **257**, 3309
Cayrel, R.: 1964, SAO *Special Report* **167**, 169
Cram, L. E.: 1977, *Astron. Astrophys.* (to be published)
Dumont, S., Heidmann, N., Kuhi, L. V., Thomas, R. N.: 1973, *Astron. Astrophys.* **29**, 199
Gingerich, O., Noyes, R. W., Kalkofen, W., Cuny, Y.: 1971, *Solar Phys.* **18**, 347
Herbig, G. H.: 1969, Liège Symposium, Pre Main Sequence Evolution, p. 13
Kalkofen, W.: 1977 (to be published)
Kalkofen, W., Ulmschneider, P.: 1977, *Astron. Astrophys.* **57**, 193
Klein, R. I., Stein, R. F., Kalkofen, W.: 1976, *Astrophys. J.* **205**, 499
Kurucz, R.: 1970, SAO Spec. Rept. 309
Kurucz, R.: 1977, *Astrophys. J. Suppl.* (to be published)
Praderie, F., Thomas, R. N.: 1976, *Solar Phys.* **50**, 333
Renzini, A., Cacciari, C., Ulmschneider, P., Schmitz, F.: 1977, *Astron. Astrophys.* (in press)
Schmitz, F., Ulmschneider, P.: 1977, *Astron. Astrophys.* **59**, 177
Schwartz, R. D.: 1974, *Astrophys. J.* **191**, 419
Smith, R. R.: 1970, Ph. D. Thesis, University of California, San Diego
Ulmschneider, P.: 1971, *Astron. Astrophys.* **14**, 275
Ulmschneider, P., Kalkofen, W., Nowak, T., Bohn, H. U.: 1977, *Astron. Astrophys.* **54**, 61
Ulmschneider, P., Kalkofen, W.: 1977, *Astron. Astrophys.* **57**, 199
Vernazza, J. E., Avrett, E. H., Loeser, R.: 1976, *Astrophys. J. Suppl.* **30**, 1